The University of Reading

A Comparison of Potential Vorticity-Based and Vorticity-Based Control Variables

D. Katz[1], A.S. Lawless[1], N.K. Nichols[1], M.J.P. Cullen[2] and R.N. Bannister[3]

NUMERICAL ANALYSIS REPORT 8/2006

[1]*Department of Mathematics*
The University of Reading
Box 220, Whiteknights
Reading, Berkshire
RG6 6AX, UK

[2]*Met Office*
FitzRoy Road
Exeter, Devon
EX1 3PB

[3]*DARC*
The University of Reading
Box 243, Earley Gate
Reading, Berkshire
RG6 6BB

Department of Mathematics

A Comparison of Potential Vorticity-Based and Vorticity-Based Control Variables

Abstract

In most operational weather forecasting centres variational data assimilation is performed using a different set of variables from the actual model variables. The transformation of variables simplifies the problem by assuming that the errors in the transformed variables are uncorrelated. The validity of this hypothesis is key to the accuracy of the data assimilation. Recently a potential vorticity (PV) based set of variables has been proposed. These new variables are thought to exploit more accurately important dynamical properties of the atmosphere. Here we present new results, obtained with a simplified 1-D shallow water model, comparing the PV-based variables to the vorticity-based variables currently used at operational weather forecasting centres, including the Met Office. The validity of the fundamental assumption that the errors in the transformed variables are uncorrelated is tested in a variety of dynamical regimes. The results show that the errors in the PV-based variables are uncorrelated across all regimes tested. This is not the case, however, for the vorticity-based variables. This suggests that the PV-based control variables imply a better representation of the background errors than the current vorticity-based variables.

1 Introduction

Data assimilation is a process for finding initial conditions for numerical weather prediction (NWP) models. By combining observational data, statistical data, knowledge of atmospheric dynamics and a previous short forecast the best estimate, or *analysis*, of the state of the atmosphere is found. Due to the chaotic nature of the governing equations any errors in the initial conditions may grow rapidly in the forecast and thus data assimilation forms a vital part of NWP. The assimilation problem is huge, with typically 10^7 variables, and special methods need to be found to make the problem practical to solve.

At the Met Office the data assimilation is performed using a different set of variables to the model variables. These variables are the control variables and the choice of these is key to the data assimilation system performance. The transformation of variables simplifies the problem by assuming that the errors in the new variables are uncorrelated. One way that is thought to do this accurately is by using *balanced* control variables. Here an attempt is made to separate the balanced and unbalanced modes as it is thought there is little or no interaction between these flows and so their errors are uncorrelated. The use of control variables in this way was first introduced in [8]. Here balance between mass and momentum is implicitly introduced by combining the balanced parts of mass and momentum fields in a single variable.

The current control variables used at the Met Office are vorticity-based and do not represent the separation of balanced and unbalanced modes in all flow regimes. Recently a new set of control variables has been proposed [2] that should be valid across all regimes. The new variables use a conserved quantity, the potential vorticity (PV), to capture the balanced mode. In [14] the PV-based approach is developed for the 2D shallow water equations on a sphere and the potential benefits are demonstrated theoretically and experimentally. These initial results are encouraging. In this study we analyse the vorticity-based and PV-based variables in the context of a simplified

1D shallow water equation model and investigate the validity of the fundamental assumption that the errors in the control variables are uncorrelated in various flow regimes.

We start by introducing the theoretical aspects of control variable transforms as they apply to four dimensional variational data assimilation (4D-VAR). We then derive the vorticity-based and PV-based transforms for the simplified shallow water equation model. In this simplified context the implications of each transform are examined. We first derive the background error covariance matrices implied by each control variable transform. This highlights a key difference between the transforms; whilst the vorticity-based transform implies static background error statistics the implied background error statistics of the PV-based transform are state-dependent. Next we test the validity of the fundamental assumption that the errors in the control variables are uncorrelated. We test whether the assumption holds as we change the dynamical regime. We also propose an approximate form of the PV-based transform and examine the consequences of this approximation on the error correlations between the approximated variables. From these results we are able to draw conclusions regarding the effectiveness of each transform.

2 Control Variable Transforms in 4D-VAR

The 4D-VAR data assimilation system allows observations to be distributed in time as well as space [6]. The goal is to find the model state $\mathbf{x}_0$ at time $t = t_0$ that minimises the cost function,

$$J[\mathbf{x}_0] = \frac{1}{2}(\mathbf{x}_0 - \mathbf{x}^b)^T \mathbf{B}^{-1}(\mathbf{x}_0 - \mathbf{x}^b) + \frac{1}{2}\sum_{i=0}^{n}(\mathcal{H}_i[\mathbf{x}_i] - \mathbf{y}_i^o)^T \mathbf{R}_i^{-1}(\mathcal{H}_i[\mathbf{x}_i] - \mathbf{y}_i^o), \quad (1)$$

with

$$\mathbf{x}_i = \mathcal{M}(t_i, t_0, \mathbf{x}_0),$$

where $\mathcal{M}(t_i, t_0, \mathbf{x}_0)$ is the non-linear model evolved to time t_i, $i = 1, \ldots, n$, $\mathbf{x}^b$ is the background field found from a previous short forecast, $\mathbf{y}_i^o$ are the observations at time $t = t_i$ and $\mathcal{H}_i$ is the observation operator that maps

model space to observational space. The background error covariance matrix is defined by $\mathbf{B}$, typically of size $O(10^7 \times 10^7)$, and $\mathbf{R}_i$ is the observation error covariance matrix, generally of size $O(10^6 \times 10^6)$. This is a non-linear least squares minimisation problem and is usually solved incrementally as discussed in [1].

Incremental 4D-VAR minimises a series of approximate convex quadratic cost functions for an increment $\mathbf{x}'_0$

$$\begin{aligned}\widetilde{J}^{(k)}[\mathbf{x}_0'^{(k)}] = \frac{1}{2}(\mathbf{x}_0'^{(k)} - \mathbf{x}'^b)^T\mathbf{B}^{-1}(\mathbf{x}_0'^{(k)} - \mathbf{x}'^b) \\ +\frac{1}{2}\sum_{i=0}^{n}(\mathbf{H}_i\mathbf{x}_i'^{(k)} - \mathbf{d}_i)^T\mathbf{R}_i^{-1}(\mathbf{H}_i\mathbf{x}_i'^{(k)} - \mathbf{d}_i),\end{aligned} \tag{2}$$

where k is the iteration count and $\mathbf{H}_i$ is the linearised observation operator. Here $\mathbf{x}_i'^{(k)} = \mathbf{M}(t_i, t_0, \mathbf{x}^{(k)})\mathbf{x}_0'^{(k)}$, where $\mathbf{M}(t_i, t_0, \mathbf{x}^{(k)}) \equiv \mathbf{M}_i$ denotes the linear evolution operator from t_0 to t_i of the tangent linear model (TLM). The TLM is a linearisation of the non-linear model about the current guess trajectory. The background increment, $\mathbf{x}'^b$, is given by $\mathbf{x}'^b = \mathbf{x}^b - \mathbf{x}_0^{(k)}$ and the innovation vector, $\mathbf{d}_i$, by $\mathbf{d}_i = \mathbf{y}_i^o - \mathcal{H}_i[\mathbf{x}_i^{(k)}]$.

Further simplification is now needed to handle the background error covariance matrix, $\mathbf{B}$, which cannot be stored in memory. This is done by transforming from model variables to new *control variables* to perform the data assimilation. The errors in these control variables are considered to be uncorrelated with each other and thus the background error covariance matrix becomes block diagonal and the size of the data assimilation problem is greatly reduced. The block components of the transformed matrix specify the auto-correlations of each variable. Effectively the problem of modelling and storing the matrix $\mathbf{B}$ is now shifted to defining the transform between state space and control space.

The transform from control variable increments, $\mathbf{z}'$, to model variable increments, $\mathbf{x}'$, is known as the U-transform,

$$\mathbf{x}' = \mathbf{U}\mathbf{z}', \tag{3}$$

and its inverse,

$$\mathbf{z}' = \mathbf{T}\mathbf{x}', \tag{4}$$

is known as the T-transform. Here $\mathbf{z}'$ are the control variable increments and $\mathbf{x}'$ the model variable increments. Substituting into the incremental cost function (2) we obtain,

$$\begin{aligned}\widetilde{J}^{(k)}[\mathbf{z}_0'^{(k)}] = \tfrac{1}{2}(\mathbf{z}_0'^{(k)} - \mathbf{z}'^b)^T\mathbf{U}^T\mathbf{B}^{-1}\mathbf{U}(\mathbf{z}_0'^{(k)} - \mathbf{z}'^b)\\ +\tfrac{1}{2}\textstyle\sum_{i=0}^{n}(\mathbf{H}_i(\mathbf{M}_i\mathbf{U}\mathbf{z}_0'^{(k)}) - \mathbf{d}_i)^T\mathbf{R}_i^{-1}(\mathbf{H}_i(\mathbf{M}_i\mathbf{U}\mathbf{z}_0'^{(k)}) - \mathbf{d}_i),\end{aligned} \tag{5}$$

where $\mathbf{U}$ is the U-transform on iteration k and $(\mathbf{M}_i\mathbf{U}\mathbf{z}_0'^{(k)})$ represents the control variable increment at the initial time transformed to model space and evolved by the TLM to time t_i. It is necessary to transform $\mathbf{z}_0'^{(k)}$ in the observation term of (5) as the linearised observation operator $\mathbf{H}_i$ and the linear model operator $\mathbf{M}_i$ act on model variables and not control variables.

If we now choose $\mathbf{U}$ such that

$$\mathbf{U}^T\mathbf{B}^{-1}\mathbf{U} = \mathbf{\Lambda}^{-1},$$

where $\mathbf{\Lambda}$ is a block diagonal matrix specifying the auto-correlations of each control variable, we imply that

$$\mathbf{B} = \mathbf{U}\mathbf{\Lambda}\mathbf{U}^T.$$

We then obtain a much simpler form of (2),

$$\begin{aligned}\widetilde{J}^{(k)}[\mathbf{z}_0'^{(k)}] = \tfrac{1}{2}(\mathbf{z}_0'^{(k)} - \mathbf{z}'^b)^T\mathbf{\Lambda}^{-1}(\mathbf{z}_0'^{(k)} - \mathbf{z}'^b)\\ +\tfrac{1}{2}\textstyle\sum_{i=0}^{n}(\mathbf{H}_i(\mathbf{M}_i\mathbf{U}\mathbf{z}_0'^{(k)}) - \mathbf{d}_i)^T\mathbf{R}_i^{-1}(\mathbf{H}_i(\mathbf{M}_i\mathbf{U}\mathbf{z}_0'^{(k)}) - \mathbf{d}_i).\end{aligned} \tag{6}$$

We remark that on each outer iteration of the incremental method, the linearized operators $\mathbf{M}_i, \mathbf{H}_i$, the transform $\mathbf{U}$ and, implicitly, the covariance $\mathbf{B} = \mathbf{U}\mathbf{\Lambda}\mathbf{U}^T$ are all updated using the current estimate of the state trajectory.

A good choice of control variables is essential as it is assumed that the errors between these variables are uncorrelated. In fact the importance of the background error covariance matrix is highlighted when only a single

observation is assimilated. Even in this simple scenario it can be shown that the analysis increment

$$\mathbf{x}^a - \mathbf{x}^b \propto \mathbf{B}(:, j) = (\mathbf{U}\mathbf{\Lambda}\mathbf{U}^T)(:, j),$$

where $\mathbf{x}^a$ is the model state at time $t = 0$ that minimises the cost function (1), $\mathbf{B}(:, j)$ is the jth column of the background error covariance matrix $\mathbf{B}$ and a single observation is located at a point j.

In order to identify possible control variables, we use dynamical properties of the system. Two types of atmospheric motion can be identified as normal modes of the primitive equations used in numerical weather prediction (NWP), linearised about a simple basic state [3]. One of these motions is slow and corresponds to a Rossby wave, whilst the others are fast and correspond to inertial-gravity waves. The slow mode is referred to as *balanced*, and the fast as *unbalanced*. This is because in the linear analysis the slow mode satisfies a linear balance condition. For the most part it is the balanced motion that is of meteorological significance. It is thought that a good choice of control variables will involve capturing the balanced and unbalanced modes in separate control variables since we assume that there is little or no interaction between these flows. In the linear case the modes evolve independently and therefore there is no interaction. In the non-linear case the degree of this interaction will depend in some sense on the degree of non-linearity.

In the following section we present the current vorticity-based control variables and an alternative version of control variables based on the potential vorticity (PV). We define the variables for a simplified form of the 1D shallow water equations (SWEs).

The vorticity-based control variables used in the Met Office data assimilation system are the streamfunction, velocity potential and 'unbalanced pressure'. Here an attempt has been made to capture the balanced part of the flow entirely by the streamfunction. A potential limitation is that the streamfunction is not the appropriate balanced variable in all flow regimes. However, the PV-based variables use a linearised form of the PV and a linear

balance relationship to define balanced and unbalanced components of the streamfunction. This change of variables should represent balance well in all regimes.

3 Model Equations

We consider the 1D SWEs given by

$$\frac{\partial u}{\partial t} + (U_c + u)\frac{\partial u}{\partial x} - fv = -g\frac{\partial (h + \widetilde{H})}{\partial x} \tag{7}$$

$$\frac{\partial v}{\partial t} + (U_c + u)\frac{\partial v}{\partial x} + fu = 0 \tag{8}$$

$$\frac{\partial h}{\partial t} + \frac{\partial h(U_c + u)}{\partial x} = 0, \tag{9}$$

where u denotes the departure of the velocity in the x-direction from a known constant forcing *mean* flow, U_c . This is a special case of the Shallow Water Equations. The model assumes that velocities u and v and the depth h do not vary in the y-direction. Here $\widetilde{H} = \widetilde{H}(x)$ is the height of the orography, f is the Coriolis parameter and g is the gravitational force. The model domain is periodic in the x-direction.

This simple model is chosen since it retains key properties of the model equations used at the Met Office and other operational centres. We have a non-trivial first-order balance relationship

$$fv - g\frac{\partial (h + \widetilde{H})}{\partial x} = 0. \tag{10}$$

This relationship is found through an asymptotic expansion in small Rossby number [9]. The Rossby number, R_o, is a dimensionless parameter

$$R_o = \frac{U}{fL}, \tag{11}$$

where U and L are characteristic velocity and length scales. It is used to measure the significance of rotation in the flow [9] and is the ratio of the inertial time scale, $\tau_1 = f^{-1}$ to the advective time scale $\tau_2 = L/U$ [3].

The balance equation is a fundamental component of both the vorticity and the PV-based transforms and is applied to increments in a linearised form. We let $u(x,t) = \bar{u}(x,t)+u'(x,t)$, $v(x,t) = \bar{v}(x,t)+v'(x,t)$ and $h(x,t) = \bar{h}(x,t) + h'(x,t)$, where $\bar{u}(x,t)$, $\bar{v}(x,t)$ and $\bar{h}(x,t)$ are reference states. If we assume that the reference states satisfy the balance equation (10) to first order accuracy, then we obtain a corresponding first-order linear balance equation for the increments, given by

$$fv' - g\frac{\partial h'}{\partial x} = 0. \tag{12}$$

The quantity

$$q = \frac{1}{h}\left(f + \frac{\partial v}{\partial x}\right), \tag{13}$$

or the potential vorticity (PV), is conserved in the simplified SWEs. It can also be shown that the simplified SWEs, linearised about a simple reference state, have three normal modes: one slow and two fast. The slow, or balanced mode satisfies linear balance and is characterised by a linearised form of the PV. The remaining two fast modes can be related to the geostrophic departure, ${}_a\zeta'$, defined by

$${}_a\zeta' = f\frac{\partial v'}{\partial x} - g\frac{\partial^2 h'}{\partial x^2}, \tag{14}$$

and the divergence

$$D' = \frac{\partial u'}{\partial x}, \tag{15}$$

where we recall that, in the system defined by (7)–(9), the model variables do not vary in the y-direction.

Another important dimensionless parameter used to characterise the flow regime is the Burger number,

$$B_u = \frac{\sqrt{gH}}{fL}, \tag{16}$$

where H is a characteristic depth scale. The Burger number is a measure of the relative importance of rotation and stratification in the flow. It is the

ratio of the Rossby number and the Froude number,

$$F_r = \frac{U}{\sqrt{gH}}. \tag{17}$$

The Froude number is the ratio of the advective velocity to the gravity wave speed, $c_g = \sqrt{gH}$. In most deep atmospheric motions F_r is small, i.e. the advective velocity is much less than the gravity wave speed.

We now derive the vorticity-based and PV-based transforms for the simplified SWE model.

3.1 Vorticity-Based Transform

The vorticity-based control variables are the streamfunction ψ', velocity potential χ' and 'unbalanced pressure' or, in the case of the SWEs, the residual unbalanced height h'_{res}. Here the rotational wind is assumed to be totally balanced. The Helmholtz decomposition is used to separate velocities into rotational and divergent parts. In 1D the Helmholtz decomposition reduces to the equations

$$\zeta' = \frac{\partial v'}{\partial x} = \frac{\partial^2 \psi'}{\partial x^2}, \tag{18}$$

and

$$D' = \frac{\partial u'}{\partial x} = \frac{\partial^2 \chi'}{\partial x^2}. \tag{19}$$

The velocities u' and v' are given by

$$u' = \frac{\partial \chi'}{\partial x}, \tag{20}$$

and

$$v' = \frac{\partial \psi'}{\partial x}. \tag{21}$$

The linearised balance relationship used in the vorticity-based transform, in terms of the increments ψ' and h', is found by differentiating (12) with respect to x and regarding all of v' as 'balanced'. Thus we obtain

$$f\frac{\partial^2 \psi'}{\partial x^2} - g\frac{\partial^2 h'_b}{\partial x^2} = 0, \tag{22}$$

where the subscript b refers to the 'balanced' part of the height variable. The streamfunction is assumed to hold all the balanced flow.

Using the vorticity equation (18) and the linear balance equation (22) the T-transform

$$\mathbf{z}' = \mathbf{T}\mathbf{x}'$$

with

$$\mathbf{x}' = \begin{pmatrix} u' \\ v' \\ h' \end{pmatrix},$$

and

$$\mathbf{z}' = \begin{pmatrix} \psi' \\ h'_{res} \\ \chi' \end{pmatrix}$$

in the context of our Shallow Water model is given by solving a sequence of equations. The method proceeds as follows:

Step 1 Solve

$$\frac{\partial^2 \psi'}{\partial x^2} = \frac{\partial v'}{\partial x} \tag{23}$$

for ψ' subject to periodic boundary conditions. The solution is unique up to an additive constant.

Step 2 Calculate the residual height h'_{res} by

$$h'_{res} = h' - h'_b = h' - \frac{f}{g}\psi', \tag{24}$$

where

$$h' = h'_b + h'_{res}.$$

The variable h'_b in equation (24) is found by integrating (22), the linear balance equation, twice to give

$$h'_b = \frac{f}{g}\psi' + c_1 x + c_2,$$

where c_1 and c_2 are constants of integration. Both ψ' and h'_b are periodic in x so $c_1 = 0$ and we choose to define the constant c_2 by $c_2 = 0$. This choice implies that the mean of h' is stored in the residual height h'_{res}.

Step 3 Solve

$$\frac{\partial^2 \chi'}{\partial x^2} = D' \tag{25}$$

for χ' subject to periodic boundary conditions. The solution is unique up to an additive constant.

Step 4 Store mean values of u' and v'. These are otherwise lost through differentiation.

Equations (23) for ψ' and (25) for χ' are solved with periodic boundary conditions. The solutions are unique up to an additive constant provided the right hand side has a zero mean value. In both cases the right hand sides are derivatives of periodic functions and therefore will always have a zero mean value. The solutions are therefore unique up to a constant and we choose this constant such that the mean value $< \psi' >$ of ψ' is zero and the mean value $< \chi' >$ of χ' is also zero, where $< \cdot >$ indicates the mean of the variable.

In solving (23) for ψ' and (25) for χ' we lose a degree of freedom by virtue of the fact that we choose ψ' and χ' to have zero mean values. However, this available degree of freedom is used to retain the mean values $< v' >$ of v' and $< u' >$ of u' that are lost through differentiation. The mean values $< v' >$ and $< u' >$ are therefore also control variables. The model variables and the vorticity-based control variables now have equal degrees of freedom.

So we see that the T-transform solves a sequence of equations producing the control variable increments given model variable increments. We now present the inverse transform, the U-transform.

Using equations (20), (21) and (22) we are able to derive the U-transform

$$\mathbf{x}' = \mathbf{U}\mathbf{z}'$$

for the simplified SWEs. Given the vorticity-based control variable increments the U-transform proceeds as follows:

Step 1 Find the velocity v' from ψ' and $< v' >$, the mean value of v'

$$v' = \frac{\partial \psi'}{\partial x} + < v' > . \tag{26}$$

Step 2 Find the balanced height increment h'_b from ψ' and calculate the full height increment h'

$$h' = h'_b + h'_{res} = \frac{f}{g}\psi' + h'_{res}. \tag{27}$$

Step 3 Find the velocity u' from χ' and $< u' >$, the mean value of u', using

$$u' = \frac{\partial \chi'}{\partial x} + < u' > . \tag{28}$$

Again a sequence of equations is solved to reconstruct the original model variables from the control variables.

It is worth noting at this point that the consideration of the mean values $< u' >$ and $< v' >$ is more natural in the implementation of the transforms at the Met Office. In the Met Office data assimilation system the transforms are performed in spectral space and only applied to wavenumbers one and above. The zero wavenumbers contain the mean values and are not transformed.

3.2 PV-Based Transform

We start by defining our variables. Again the Helmholtz decomposition is used to separate velocities into rotational and divergent parts. In 1D the Helmholtz decomposition reduces to equations (18) to (21). Additionally we let $h' = h'_b + h'_u$ and $v' = v'_b + v'_u$ imply $\psi' = \psi'_b + \psi'_u$, where the subscripts refer to the balanced and unbalanced parts of the variable. So we have

$$v'_b = \frac{\partial \psi'_b}{\partial x} \tag{29}$$

and

$$v'_u = \frac{\partial \psi'_u}{\partial x}. \tag{30}$$

Splitting the velocity v' in this manner allows for balanced and unbalanced components of the rotational wind. Therefore not all the rotational wind is assumed balanced, unlike the case with the vorticity-based variables.

We define the reference PV for our simplified model as in [13], giving

$$\bar{q} = \frac{1}{\bar{h}} \left(f + \frac{\partial \bar{v}}{\partial x} \right), \tag{31}$$

where the reference states $\bar{v}, \bar{h}$ and $\bar{q}$ are either the first guess, or background states, on the first outer loop of the incremental 4D-VAR, or updates to the background on subsequent outer loops.

For the PV-based transform we define the balanced variables v_b' and h_b' such that they satisfy the linear balance equation

$$fv_b' - g\frac{\partial h_b'}{\partial x} = 0 \tag{32}$$

and the linearised PV equation. To derive the linearised PV equation we follow [13] and start by linearising (31) around a varying reference state

$$q(x,t) = \bar{q}(x,t) + q'(x,t)$$

$$v(x,t) = \bar{v}(x,t) + v'(x,t)$$

$$h(x,t) = \bar{h}(x,t) + h'(x,t),$$

where the overbar denotes the reference state and the prime is a perturbation to it. This gives

$$q = \frac{1}{h}\left(f + \frac{\partial v}{\partial x}\right) = \frac{1}{\bar{h}+h'}\left(f + \frac{\partial \bar{v}}{\partial x} + \frac{\partial v'}{\partial x}\right).$$

Therefore, neglecting products of the perturbations, we have to first order accuracy

$$\bar{q}\bar{h} + q'\bar{h} + \bar{q}h' = f + \frac{\partial \bar{v}}{\partial x} + \frac{\partial v'}{\partial x},$$

and then, using equation (31), we obtain

$$q'\bar{h} = \frac{\partial v'}{\partial x} - \bar{q}h'. \tag{33}$$

Since we assume that the balanced variables v_b' and h_b' satisfy the linearised PV equation (33) for q', we have

$$\frac{\partial v_b'}{\partial x} - \bar{q}h_b' = q'\bar{h}. \tag{34}$$

There are also corresponding equations for the unbalanced variables. We define the unbalanced variables $v_u' = v' - v_b'$ and $h_u' = h' - h_b'$ such that they satisfy the departure from linear balance equation

$$fv_u' - g\frac{\partial h_u'}{\partial x} = fv' - g\frac{\partial h'}{\partial x}, \tag{35}$$

and

$$\frac{\partial v'_u}{\partial x} - \bar{q}h'_u = 0, \tag{36}$$

i.e. the unbalanced variables do not contribute to the PV increment.

Re-writing these equations using the balanced and unbalanced stream-functions ψ'_b and ψ'_u gives the following four equations

$$\begin{aligned}
f\frac{\partial^2\psi'_b}{\partial x^2} - g\frac{\partial^2 h'_b}{\partial x^2} &= 0, & (37)\\
\frac{\partial^2\psi'_b}{\partial x^2} - \bar{q}h'_b &= q'\bar{h}, & (38)\\
f\frac{\partial^2\psi'_u}{\partial x^2} - g\frac{\partial^2 h'_u}{\partial x^2} &= {}_a\zeta', & (39)\\
\frac{\partial^2\psi'_u}{\partial x^2} - \bar{q}h'_u &= 0, & (40)
\end{aligned}$$

where ${}_a\zeta'$ is defined by (14). These equations, with appropriate boundary conditions specified later in this report, define four variables ψ'_b, ψ'_u, h'_b and h'_u.

We can now derive the PV-based transform in the context of the model (7) to (9) using equations (37) to (40) and the divergence equation (19). We have five variables $\psi'_b, \psi'_u, h'_b, h'_u$ and χ'. From these we must choose the appropriate number of analysis variables. There must be two unbalanced variables and one balanced variable. However, our choice of variables must result in a well conditioned U-transform. With this in mind we choose ψ'_b as our balanced variable, since this avoids dividing through by f. This would be an issue when the equations are solved on a sphere, as f goes to zero on the equator. One of our unbalanced variables must be χ' and our remaining unbalanced variable we choose to be the unbalanced height, h'_u. Whilst theoretically it is an equivalent choice to use ψ'_u instead of h'_u, it is found that this choice can affect the numerical efficiency of the transform [2].

Using equations (37) to (40) and (19) the T-transform

$$\mathbf{z}' = \mathbf{T}\mathbf{x}'$$

with

$$\mathbf{x}' = \begin{pmatrix} u' \\ v' \\ h' \end{pmatrix},$$

and

$$\mathbf{z}' = \begin{pmatrix} \psi_b' \\ h_u' \\ \chi' \end{pmatrix}$$

is given by solving the following sequence of equations:

Step 1 Solve

$$\frac{\partial^2 \psi_b'}{\partial x^2} - \frac{f\bar{q}}{g}\psi_b' = q'\bar{h} \tag{41}$$

for ψ_b' subject to periodic boundary conditions. The right hand side is known from the model variable increment fields. The equation has a unique solution provided $\bar{q} > 0$.

Step 2 Solve

$$f\bar{q}h_u' - g\frac{\partial^2 h_u'}{\partial x^2} = {}_a\zeta' \tag{42}$$

for h_u' subject to periodic boundary conditions. As before the right hand side is known from the model variable increment fields and the equation has a unique solution provided $\bar{q} > 0$.

Step 3 Solve

$$\frac{\partial^2 \chi'}{\partial x^2} = D' \tag{43}$$

for χ' subject to periodic boundary conditions. The solution is unique up to an additive constant.

Step 4 Store mean values of u' and v'. These are otherwise lost through differentiation.

Equation (41) is found by substituting $h_b' = \frac{f}{g}\psi_b'$ from (37), the linear balance equation, into equation (38). Here we have integrated (37) twice with both constants of integration defined to be zero, as was done for the

Met Office variables. Equation (42) is found by substituting $\nabla^2\psi'_u$ from equation (40) into equation (39).

Equation (43) is solved with periodic boundary conditions for χ' and has a unique solution up to an additive constant provided the right hand side has a zero mean value. The right hand side is a derivative of a periodic function and therefore will always have a zero mean value. The solution is therefore unique up to a constant and we choose this constant such that the mean value $< \chi' >$ is zero. We therefore lose a degree of freedom in χ'. However, we use this available degree of freedom to retain the mean value $< u' >$ that is lost through differentiation. We also note that a degree of freedom in $\psi' = \psi'_b + \psi'_u$ is lost since the unbalanced streamfunction ψ'_u is found by solving (40) i.e.

$$\frac{\partial^2 \psi'_u}{\partial x^2} = \bar{q} h'_u \tag{44}$$

subject to periodic boundary conditions. The right hand side is known and must have a mean value of zero for the equation to have a solution. Provided that this is true the solution ψ'_u is unique up to an additive constant, chosen to be zero. Thus, we again lose a degree of freedom. However, this available degree of freedom is used to store the mean value $< v' >$. The degrees of freedom in both the control variables and the model variables are now equal. Again, as with the vorticity-based variables, the mean values $< u' >$ and $< v' >$ are also control variables.

We note from equation (42) that if we first apply the T-transform to our model variable increments we will always produce h'_u such that the mean of $\bar{q}h'_u$ is zero. However, the T-transform is not applied before the U-transform in the incremental 4D-VAR algorithm since the inner minimisation is performed *in control space*. This issue is addressed later in this section. However, first we present the inverse transform, the U-transform, in the context of our simplified SWEs.

Using equations (20), (29), (30), (37) and (40) we are able to derive the U-transform

$$\mathbf{x}' = \mathbf{U}\mathbf{z}'$$

for the simplified SWEs. Given the PV-based control variable increments the U-transform proceeds as follows:

Step 1 Find the balanced velocity increment v'_b from ψ'_b using

$$v'_b = \frac{\partial \psi'_b}{\partial x}. \tag{45}$$

Step 2 Find the unbalanced velocity increment v'_u from ψ'_u using

$$v'_u = \frac{\partial \psi'_u}{\partial x}, \tag{46}$$

where ψ'_u is found by solving

$$\frac{\partial^2 \psi'_u}{\partial x^2} = \bar{q} h'_u,$$

subject to periodic boundary conditions. The right hand side is known and must have a mean value of zero for the equation to have a solution. Provided that this is true, the solution ψ'_u is unique up to an additive constant.

Step 3 Reconstruct the full velocity increment

$$v' = v'_b + v'_u + < v' >, \tag{47}$$

where $< v' >$ is the mean value of v'.

Step 4 Find the balanced height increment h'_b from ψ'_b and reconstruct the full height increment

$$h' = h'_b + h'_u = \frac{f}{g}\psi'_b + h'_u. \tag{48}$$

Step 5 Find the velocity u' from χ' and $< u' >$ using

$$u' = \frac{\partial \chi'}{\partial x} + < u' > . \tag{49}$$

So the U-transform solves a series of equations reconstructing model variable increments from the control variable increments. We must now consider

the practical implementation of the U-transform in the incremental 4D-VAR algorithm.

In equation (46) the unbalanced streamfunction ψ'_u is found by solving (44). The right hand side of (44) is known and must have a mean value of zero for the equation to have a solution. In the optimisation algorithm we minimise the cost function in control space and therefore the condition that the mean of $\bar{q}h'_u$ is zero may not be satisfied unless explicitly enforced. It is not straightforward to do this, since $\bar{q}$ is varying in x and is modified on every outer iteration. However, it is possible to adjust the mean of h'_u, $< h'_u >$, on *each inner iteration* so that $< \bar{q}h'_u >$ is zero. This can be achieved since we are always able to subtract a constant from h'_u such that $< \bar{q}h'_u >$ is zero. Note that it is not a simple case of setting $< h'_u >= 0$; $< h'_u >$ will be non-zero and change on each inner iteration. The constant then must be added to h'_b to preserve the degrees of freedom in h'. The mean of the full height increment is therefore split between h'_b and h'_u.

The problem could be avoided by choosing to approximate $\bar{q}$ by a constant. An approximation of this sort was made in [2]. In the simplified SWEs context this would mean that we are simply able to explicitly set $< h'_u >= 0$ and so $\bar{q}h'_u$ will always have a zero mean value. We then store the mean of the full height increment solely in h'_b. This approximation is also desirable from an operational perspective since the transform would be less computationally demanding. In the following section we consider the possible implications of making this approximation in the PV-based transform. We note that approximating $\bar{q}$ to any constant would achieve this type of simplification. We therefore choose to approximate $\bar{q} = f/ < \bar{h} >$, where $< \bar{h} >$ is the mean of the linearisation state fluid depth.

4 Analysis of Vorticity and PV-Based Transforms

In [13], [14] it was found that for the simplified SWEs the relative contributions to the scaled PV increment, given (from equation (33)) by

$$\frac{q'}{\bar{q}} = \frac{\frac{\partial v'}{\partial x}}{f + \frac{\partial \bar{v}}{\partial x}} - \frac{h'}{\bar{h}},$$

change with the Burger number. In a high Burger regime the scaled PV increment is dominated by absolute vorticity increments and in a low Burger regime the height increments dominate. This suggests that the vorticity-based variables will capture the balanced motion well in a high Burger regime but will fail to do so in the low Burger case. This is because all the rotational wind is assumed to be balanced. On the other hand the PV-based variables allow an unbalanced rotational wind and should therefore represent the balanced and unbalanced motion well in both Burger regimes.

In the following experiments we attempt to verify this hypothesis. We examine the error correlations between the control variables in both high and low Burger regimes using some basic statistical experiments. However, we start by first deriving the background error statistics implied by each transform. This highlights a key difference between the vorticity and the PV-based transforms.

4.1 Implied Background Error Covariance Statistics

Using the above transforms we are able to derive the implied background error statistics using

$$\mathbf{B} = \mathbf{U}\mathbf{\Lambda}\mathbf{U}^T.$$

In the following analysis, for ease of notation, we do not consider the mean values of the increments u' and v'.

For the vorticity-based variables using $\mathbf{U}$ as defined by (26) to (28) we have

$$\begin{pmatrix} u' \\ v' \\ h' \end{pmatrix} = \begin{pmatrix} \frac{\partial}{\partial x} & 0 & 0 \\ 0 & \frac{\partial}{\partial x} & 0 \\ 0 & \frac{f}{g} & 1 \end{pmatrix} \begin{pmatrix} \chi' \\ \psi' \\ h'_{res} \end{pmatrix}$$

and therefore

$$\mathbf{B}_V = \begin{pmatrix} \left(\frac{\partial}{\partial x}\right) \mathbf{\Lambda}_\chi \left(\frac{\partial}{\partial x}\right)^T & 0 & 0 \\ 0 & \left(\frac{\partial}{\partial x}\right) \mathbf{\Lambda}_\psi \left(\frac{\partial}{\partial x}\right)^T & \left(\frac{\partial}{\partial x}\right) \mathbf{\Lambda}_\psi \frac{f}{g} \\ 0 & \left(\left(\frac{\partial}{\partial x}\right) \mathbf{\Lambda}_\psi \frac{f}{g}\right)^T & \left(\frac{f}{g}\right)^2 \mathbf{\Lambda}_\psi + \mathbf{\Lambda}_{h_r} \end{pmatrix},$$

where $\mathbf{\Lambda}_\chi, \mathbf{\Lambda}_\psi$ and $\mathbf{\Lambda}_{h_r}$ are the auto-correlation matrices for χ', ψ' and h'_{res} respectively.

For PV-based control variables $\mathbf{U}$ is given by (45) to (47). This implies

$$\begin{pmatrix} u' \\ v' \\ h' \end{pmatrix} = \begin{pmatrix} \frac{\partial}{\partial x} & 0 & 0 \\ 0 & \frac{\partial}{\partial x} & \mathbf{Q} \\ 0 & \frac{f}{g} & 1 \end{pmatrix} \begin{pmatrix} \chi' \\ \psi'_b \\ h'_u \end{pmatrix},$$

where $\nabla^2 \equiv \frac{\partial^2}{\partial x^2}$, and the implied background error covariance matrix is therefore

$$\mathbf{B}_{PV} = \begin{pmatrix} \left(\frac{\partial}{\partial x}\right) \mathbf{\Lambda}_\chi \left(\frac{\partial}{\partial x}\right)^T & 0 & 0 \\ 0 & \left(\frac{\partial}{\partial x}\right) \mathbf{\Lambda}_{\psi_b} \left(\frac{\partial}{\partial x}\right)^T + \mathbf{Q}\mathbf{\Lambda}_{h_u}\mathbf{Q}^T & \left(\frac{\partial}{\partial x}\right) \mathbf{\Lambda}_{\psi_b} \frac{f}{g} + \mathbf{Q}\mathbf{\Lambda}_{h_u} \\ 0 & \left(\left(\frac{\partial}{\partial x}\right) \mathbf{\Lambda}_{\psi_b} \frac{f}{g} + \mathbf{Q}\mathbf{\Lambda}_{h_u}\right)^T & \left(\frac{f}{g}\right)^2 \mathbf{\Lambda}_{\psi_b} + \mathbf{\Lambda}_{h_u} \end{pmatrix},$$

where the operator $\mathbf{Q}$ is given by

$$\mathbf{Q} = \left(\frac{\partial}{\partial x}\left(\nabla^{-2}\bar{q}\ \cdot\right)\right),$$

and $\mathbf{\Lambda}_\chi, \mathbf{\Lambda}_{\psi_b}$ and $\mathbf{\Lambda}_{h_u}$ are the auto-correlation matrices for χ', ψ'_b and h'_u respectively.

A comparison of $\mathbf{B}_V$ and $\mathbf{B}_{PV}$ shows that the differences between the implied background error statistics are the covariances $COV(v', h')$,

$COV(h', h')$ and $COV(v', v')$. The statistical model is much more complicated for the PV-based variables and, whilst $\mathbf{B}_V$ is static, the PV-based implied background error statistics include the linearised PV $\bar{q}$. Thus the PV-based transforms have introduced state-dependence into the implied background error statistics.

4.2 The Correlation of Control Variables

We now test the assumption that the errors in the vorticity and PV-based control variables are uncorrelated. If the control variables are indeed representing the balanced and unbalanced flows, then we should see very little correlation between the balanced and unbalanced variables. However, if the vorticity-based variables are not representing the balanced flow well in the low Burger regime we would expect to see a correlation between ψ' and h'_{res}.

We are also in a position to consider the consequences of using an approximate $\bar{q} = f/ < \bar{h} >$ in the PV-based transforms. This can be achieved by looking at the correlation of the approximated PV-based variables.

We start by briefly introducing the two-time-level semi-implicit, semi-Lagrangian (SISL) scheme used to solve the simplified SWEs.

4.2.1 The Discrete Model Equations

The simplified SWEs, equations (7) to (9), are written in terms of their full Lagrangian derivatives as follows,

$$\frac{Du}{Dt} + \phi_x + g\widetilde{H}_x - fv = 0, \tag{50}$$

$$\frac{Dv}{Dt} + fu = 0, \tag{51}$$

$$\frac{D \ln \phi}{Dt} + u_x = 0, \tag{52}$$

where

$$\frac{D}{Dt} \equiv \frac{\partial}{\partial t} + (U_c + u)\frac{\partial}{\partial x}$$

and

$$\phi = gh.$$

This form of the equations is chosen as it is a more convenient when applying the SISL scheme [11].

Applying the SISL scheme as in [5] to the equations (50)–(52) gives the following time-discrete equations

$$\frac{u_a^{n+1} - u_d^n}{\Delta t} + \alpha_1 \left[\phi_x + g\widetilde{H}_x - fv\right]_a^{n+1} + (1-\alpha_1)\left[\phi_x + g\widetilde{H}_x - fv\right]_d^n = 0, \quad (53)$$

$$\frac{v_a^{n+1} - v_d^n}{\Delta t} + \alpha_2 \left[fu\right]_a^{n+1} + (1-\alpha_2)\left[fu\right]_d^n = 0, \quad (54)$$

$$\frac{\ln \phi_a^{n+1} - \ln \phi_d^n}{\Delta t} + \alpha_3 \left[u_x\right]_a^{n+1} + (1-\alpha_3)\left[u_x\right]_d^n = 0, \quad (55)$$

where the subscript x denotes the derivative with respect to x, and the superscript denotes the value at time level n. The constants $\alpha_1, \alpha_2, \alpha_3$ are chosen to meet the stability requirements of the scheme. The advection terms are time differences along trajectories and *all* other terms are time averages along trajectories. The Coriolis terms are treated in this way as this avoids the introduction of instability due to using extrapolated values to evaluate the Coriolis terms [11]. The subscripts a and d represent the arrival and departure points.

Equations (53)–(55) are solved on a staggered grid, which is a 1D analogue of the Arakawa B-grid. The grid has ϕ on x_i points and u and v on $x_{i+1/2}$ points. Firstly the departure points are found iteratively as in [11]. We can assume that we know all values at all grid points at time n and therefore by interpolating to the departure points we may find all the terms at t_n in the equations (53)–(55). We then write these equations with all known terms on the right hand side. We may then eliminate u_a^{n+1} and v_a^{n+1} by substitution and solve an elliptic equation for ϕ_a^{n+1} as in [5]. Now that we have ϕ_a^{n+1} we can substitute back to find u_a^{n+1} and v_a^{n+1}, hence completing one time step.

For the following experiments the model domain has $N = 500$ grid points with grid spacing $\Delta x = 12.5m$. The time step $\Delta t = 2.5s$ and the Coriolis

parameter $f = 0.01\text{s}^{-1}$. The orography is given by

$$\widetilde{H}(x) = H_c\left(1 - \frac{x^2}{a^2}\right) \quad \text{for} \quad -a \leq x \leq a \tag{56}$$

$$= 0 \quad \text{otherwise} \tag{57}$$

with $a = 40\Delta x$, $H_c = 7.6m$ in the high Burger regime and $H_c = 0.019m$ in the low Burger regime. For the high Burger experiments the mean depth $< h > \approx 40m$ and for the low Burger experiments $< h > \approx 0.1m$.

4.2.2 Correlation Experiment: Method

It is assumed in the data assimilation that the errors in the control variables are uncorrelated. We now investigate the truth of this assumption. We look at correlations of the errors in the vorticity and PV-based control variables where we fix the Burger number to be either high or low and vary the Rossby number. We also try to assess the effect of using an approximate $\bar{q} = f/< \bar{h} >$ on the correlation between errors in the PV-based control variables.

We start by assuming that background errors are similar to forecast errors. This assumption is made since the background field in operational centres is a previous short forecast.

There are many ways to obtain forecast error statistical data. A popular example is the NMC method, as described in [8]. The NMC method assumes that the spatial correlations of background errors are similar to the correlations of differences between 24 hour and 48 hour forecasts *valid at the same time*. Forecast times are taken 24 hours apart to remove the diurnal signal, which would otherwise dominate the statistics. This method is fairly complicated and time consuming to implement. Therefore for initial analysis we choose to use a much simpler approach based on the Canadian Meteorological Centre's 'quick-covs' method [10]. Here we generate a single long forecast using our model. We then take forecast differences at regular time intervals apart. This is done until we have a data set of multiple time differences. Using these differences we may look at the correlations of the difference fields. We can examine the correlation between errors in control

variables by transforming the forecast time-differences using the relevant T-transform; either equations (23) to (25) for the vorticity-based transforms or equations (41) to (43) for the PV-based transforms.

We then look at the covariance $COV(\psi', h')$ and $COV(\psi, h + \widetilde{H})$ for model fields, where the primes indicate difference fields, and ψ and $h + \widetilde{H}$ are full forecast fields with $h + \widetilde{H}$ being the total height of the free surface. We are primarily concerned with covariance of these specific variables since they are related through the balance equations (10) and (12). The covariance $COV(\psi', h')$ tells us about the balance in the time-difference fields and $COV(\psi, h + \widetilde{H})$ tells about the balance in the full fields. The aim of the control variable transform is to decorrelate these variables. We therefore also look at the covariance $COV(\psi', h'_{res})$ and $COV(\psi'_b, h'_u)$ to test this assumption, where $COV(\psi', h'_{res})$ and $COV(\psi'_b, h'_u)$ are the covariances of errors in the vorticity and PV-based variables respectively. We also then compare $COV(\psi'_b, h'_u)$ with $COV(\psi'_b, h'_u)$ when the approximate PV $\bar{q} = f/ < h >$ is used in the PV-based transform.

Covariances are calculated by treating each component of each vector as equivalent to one realisation of a single random variable. We thus obtain a set of $N \times M$ realisations of each random variable, where N is the number of points in the domain and M is the number of time differences; for example, we have

$$\psi = \left\{ \psi_1^1, \ldots, \psi_N^1, \psi_1^2, \ldots, \psi_N^2, \ldots\ldots, \psi_1^M, \ldots, \psi_N^M \right\}, \tag{58}$$

where the subscript indicates the grid point and the superscript the forecast difference field.

The error covariances are then computed from

$$COV(\psi', h') =< (\psi' - < \psi' >)(h' - < h' >) >=< \psi' h' > - < \psi' >< h' >, \tag{59}$$

where $< h' >$, $< \psi' >$ are the mean values of h' and ψ' given by

$$< h' >= \frac{h'_1 + \ldots + h'_{N \times M}}{N \times M}, \tag{60}$$

and

$$< \psi' >= \frac{\psi'_1 + \ldots + \psi'_{N\times M}}{N \times M}; \tag{61}$$

also

$$< \psi' h' >= \frac{(\psi'_1 h'_1 + \ldots + \psi'_{N\times M} h'_{N\times M})}{N \times M}. \tag{62}$$

We then calculate the correlation coefficient

$$\rho_{\psi h} = \frac{COV(\psi', h')}{\sigma_{\psi'}\sigma_{h'}}, \tag{63}$$

where the σ represents the standard deviations of ψ' and h', and

$$\sigma_{h'} = \sqrt{(< (h' - < h' >)^2 >)} = \sqrt{(< h'^2 > - < h' >^2)} \tag{64}$$

with

$$< h'^2 >= \frac{h'^2_1 + \ldots + h'^2_{N\times M}}{N \times M}. \tag{65}$$

The standard deviation of ψ' is calculated in the same way. The correlation coefficient varies

$$-1 \leq \rho_{\psi h} \leq 1,$$

with $\rho_{\psi h}$ close to 1 or -1 indicating strong positive or negative correlation between ψ' and h'. A value of $\rho_{\psi h}$ close to 0 indicates that the variables are uncorrelated. This is repeated for each pair of variables and gives correlation coefficients for each forecast time difference and for the full fields.

4.2.3 Correlation Experiment: Time-difference interval

The method is very sensitive to the length of the time-difference interval used, as is the NMC method. In the NMC method, the interval is taken to be one day in order to remove the diurnal signal. The 'quick-covs' method used in [10] takes 6 hour difference fields since the background state is a 6 hour forecast. The difference fields are then adjusted to remove the diurnal signal. In our model the dominant signal is different. The dominant signal in our model is artificially produced due to the periodic boundary conditions.

In the high Burger case the fast gravity waves cover the length of the domain in time $\frac{N\Delta x}{\sqrt{gH}}s$. We choose to remove this signal from the time-difference fields by choosing a time interval of $\frac{N\Delta x}{\sqrt{gH}}s$.

In the low Burger number experiments the dominant gravity wave is actually stationary and tied to the orography, as we discuss in Section 4.2.5. We are therefore free to choose the sampling period in this case, and choose the same period as used in the high Burger case.

4.2.4 Correlation Experiment: High Burger Regime

The results for the high Burger regime are presented in figure 1, where the correlation coefficient is plotted against the Rossby number for each pair of variables. Figure 1 shows a strong correlation between model variables in the full fields $(\psi, h + \widetilde{H})$ and the difference fields (ψ', h'). This correlation increases as the Rossby number decreases and the flow becomes increasingly balanced.

The correlation for the vorticity-based variables (ψ', h'_{res}) and PV-based variables (ψ'_b, h'_u) is much less and very similar for $R_o < 0.5$. However, as the Rossby number increases above $R_o = 0.5$ we notice that the correlation of the PV-based variables also increases slightly whilst the vorticity-based variables correlations stay relatively constant. This increase in the correlation of the PV-variables can be attributed to the fact that as R_o increases the flow is becoming increasingly non-linear. Thus the linear approximations used in the PV-based transform are becoming less accurate. However, this increase is slight and the PV-based variables are still significantly more uncorrelated than the model variables.

In figure 1 the correlation between PV-based variables when we use an approximate $\bar{q} = f/ < \bar{h} >$ is almost identical to the correlation when the full PV is used.

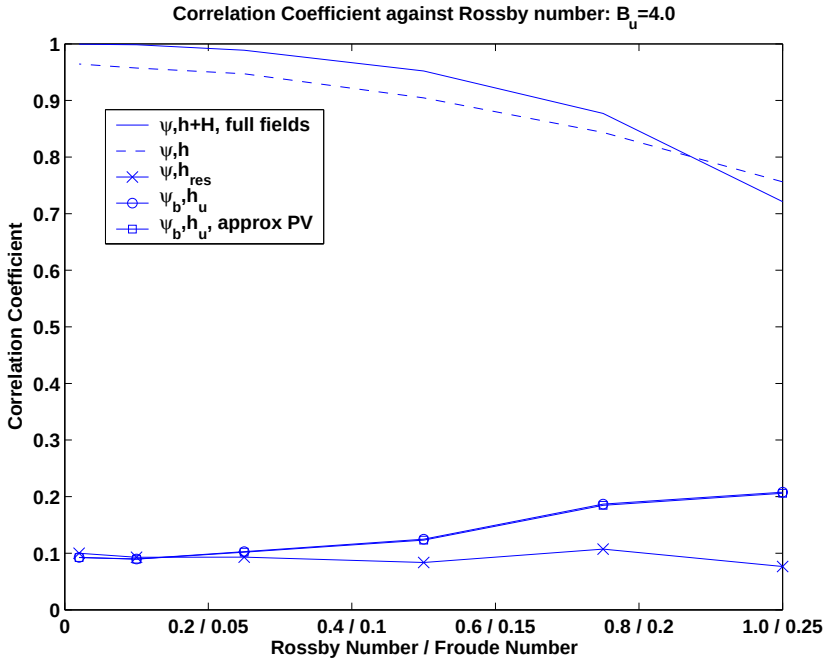

Figure 1: Plot of correlation coefficient against Rossby number for $B_u = 4.0$. The solid line is the correlation for full model field ψ and $h + \widetilde{H}$, the dashed line for model field time differences ψ' and h'. Vorticity-based control variable correlations ψ' with h'_{res} are indicated with the crosses and PV-based variables ψ'_b with h'_u using the full $\bar{q}$ are circles and the approximate $\bar{q} = f/ < \bar{h} >$, squares.

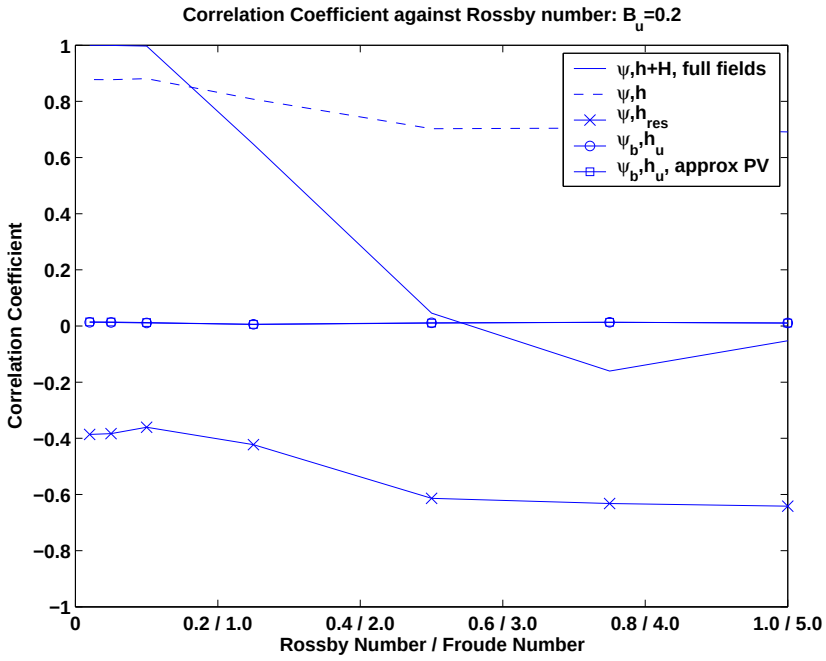

Figure 2: Plot of correlation coefficient against Rossby number for $B_u = 0.2$. The solid line is the correlation for full model field ψ and $h + \widetilde{H}$, the dashed line for model field time differences ψ' and h'. Vorticity-based control variable correlations ψ' with h'_{res} are indicated with the crosses and PV-based variables ψ'_b with h'_u using the full $\bar{q}$ are circles and the approximate $\bar{q} = f/ < \bar{h} >$, squares.

4.2.5 Correlation Experiment: Low Burger Regime

The low Burger regime experiment results are presented in figure 2 where again the correlation coefficient is plotted against the Rossby number. We see in figure 2 that the PV-based variables are still uncorrelated. The vorticity-based variables, however, show a strong negative correlation. Both these correlations seem to be independent of Rossby number.

As the Rossby number decreases the correlations between the full fields increase as in the high Burger experiment. However, this time the correlation of the variables (ψ', h') remains relatively unaffected by changes in the Rossby number. This behaviour is caused by a stationary wave in the forecast fields

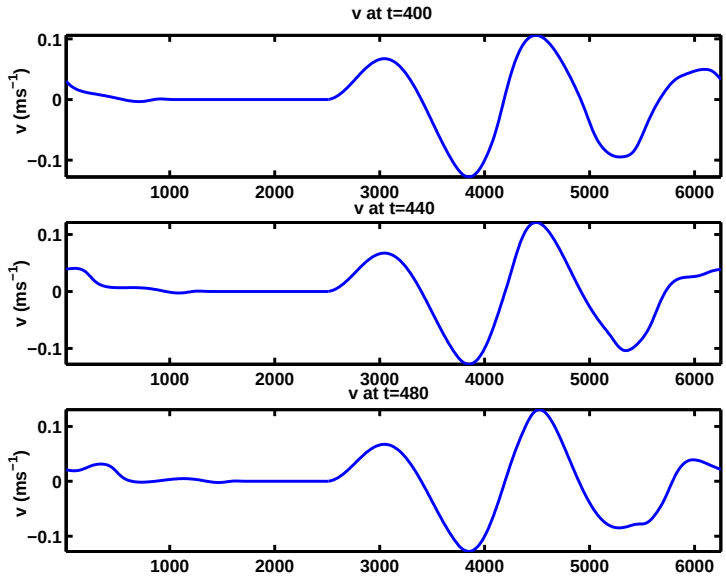

Figure 3: Plots show stationary wave in v for times one inertial period apart.

that is tied to the orography. The wave is not seen in the time-difference fields but does have a signal in the full field correlations. This can be seen in figure 3 where the full v-field is plotted at several different times in the forecast run. The stationary wave becomes increasingly balanced as the Rossby number decreases.

As in the high Burger experiment, the correlation of the errors in the PV-based variables where we use an approximate PV is in good agreement with the correlation when the full PV is used. This can be seen in figure 2 where the correlations are almost indistinguishable.

These results give strong evidence that the PV-based variables are able to separate the flow accurately into balanced and unbalanced parts and further that this separation is uncorrelated. This suggests that the PV-based variables should be a much better choice of control variables than the current vorticity-based variables in a low Burger regime. Making the approximation $\bar{q} = f/ < \bar{h} >$ has very little effect on the correlation of the errors in the PV-based variables.

5 Summary and Conclusions

Control variable transforms in data assimilation have a dual function. Firstly they are a necessity due to the size of the background error covariance matrix. Secondly, they are used to introduce important physical relationships into the data assimilation. We show how the control variable transform is used in 4D-VAR and that the key assumption is that the errors in the control variables are uncorrelated. This simplifies the data assimilation problem but also implicitly models the background errors as

$$\mathbf{B} = \mathbf{U}\mathbf{\Lambda}\mathbf{U}^T.$$

We then derive two sets of control variables for a simplified SWE model, the vorticity-based and the PV-based versions, which attempt to exploit properties of balance. We are then able to derive, in this simple case, the implied background statistics for each transform. This highlights several key differences in the two transforms. Most importantly that the implied background statistics for the vorticity-based transforms are static whilst the PV-based transforms are state-dependent as they involve the linearised form of the PV.

We then test the assumption that the errors in the control variables are uncorrelated. We are able to validate our hypothesis that the PV-based variables capture the balanced motion in both high and low Burger regimes, whilst the vorticity-based transforms fail in the low Burger regime. This suggests that the PV-based control variables are a much better choice than the vorticity-based variables.

We also consider a possible approximation to the linearisation state PV, which forms part of the PV-based transform. By approximating

$$\bar{q} = f / < \bar{h} >$$

we are able to simplify the implementation of the transform. We demonstrate that making this approximation has little or no effect on the correlations of the PV-based variables.

These results suggest that the PV-based variables are superior to the vorticity-based variables in several vital areas: the PV-based variables imply a state-dependent matrix B and the assumption that the errors in the PV-based variables are uncorrelated is valid in all regimes tested.

The obvious next step is to compare control variables in assimilation experiments. This would involve identical twin 4D-VAR experiments using single and incomplete sets of observations. The success of the experiment should be assessed against how well the balanced flow is represented in the analysis. To do this we can look at the PV in each analysis and compare this to the true PV. This work is currently being carried out as part of a PhD research project and will be published in a subsequent report.

Acknowledgements

This research was supported in part by a UK Engineering and Physical Sciences Research Council CASE Studentship in collaboration with the Met Office and by the UK Natural Environment Research Council.

References

[1] P. Courtier, J. Thepaut and A. Hollingsworth: A strategy for operational implementation of 4D-Var, using an incremental approach. *Quart. J. Royal Met. Soc.*, 120:pp. 1367-1387 (1994)

[2] M. J. P. Cullen: Four-dimensional variational data assimilation: A new formulation of the background-error covariance matrix based on a potential vorticity representation. *Quart. J. Royal Met. Soc.*, 129:pp. 2777-2796 (2003)

[3] R. Daley: Atmospheric Data Analysis. *Cambridge University Press* (1993)

[4] C. Johnson: PhD Thesis: Information Content of Observations in Variational Data Assimilation. *University of Reading* (2003)

[5] A. S. Lawless, N. K. Nichols and S. P. Ballard: A comparison of two methods for developing the linearization of a shallow water model. *Quart. J. Royal Met. Soc.*, 129:pp. 1237-1254 (2003)

[6] F. X. Le Dimet and O. Talagrand, Variational algorithms for analysis and assimilatin of meteorological observations. *Tellus*, 38A:pp. 97-110 (1986)

[7] A. R. Mohebalhojeh and D. G. Dritschel: Hierarchies of Balance Conditions for the f-plane Shallow Water Equations. To be published in *Journal of the Atmospheric Sciences*

[8] D. Parrish and J. C. Derber: The National Meteorological Center's Spectral Statistical-Interpolation Analysis System. *Monthly Weather Review*, 120:pp. 1747-1763 (1992)

[9] J. Pedlosky: *Geophysical Fluid Dynamics*, Springer-Verlag (1979)

[10] S. Polavarapu, S. Ren, Y. Rochon, D. Sankey, N. Ek, J. Koshyk and D. Tarasick: Data Assimilation with the Canadian Middle Atmosphere Model. *Atmosphere-Ocean* 43(1):pp. 77-100 (2005)

[11] Andrew Staniforth and Jean Cote: Semi-Lagrangian integration schemes for atmospheric models - A review. *Monthly Weather Review* volume 119:pp. 2206-2223 (1991)

[12] A. Weaver and P. Courtier: Correlation modelling on the sphere using a generalized diffusion equation. *Quart. J. Royal Met. Soc.*, 127:pp. 1815-1846 (2001)

[13] M. Wlasak: The examination of balanced and unbalanced flow using Potential Vorticity in Atmospheric Modelling. *PhD Thesis, University Of Reading* (2002)

[14] M. Wlasak: Use of Potential Vorticity for Incremental Data Assimilation. *University Of Reading, Department of Mathematics, Numerical Analysis Report NA 1/2006* (2006)